BIOCHEMISTRY
including biophysical chemistry & molecular biology

Article

pubs.acs.org/biochemistry

Kinetic Studies of a Ferredoxin-Dependent Cyanobacterial Nitrate Reductase

Anurag P. Srivastava,[†] David B. Knaff,*[,†,‡] and Pierre Sétif[§]

[†]Department of Chemistry and Biochemistry, Texas Tech University, Lubbock, Texas 79409-1061, United States
[‡]Center for Biotechnology and Genomics, Texas Tech University, Lubbock, Texas 79409-3132, United States
[§]iBiTec-S, CNRS UMR 8221, CEA Saclay, 91191 Gif-sur-Yvette, France

Supporting Information

ABSTRACT: A flash photolysis study of electron transfer (ET) kinetics from reduced ferredoxin (photoreduced by Photosystem I) to the ferredoxin-dependent nitrate reductase from the cyanobacterium *Synechococcus* sp. PCC 7942 has been carried out. In the presence of nitrate, under conditions where only a single electron is transferred to nitrate reductase, the rate of enzyme reduction shows a biphasic concentration dependence: At low enzyme concentrations the dependence is approximately linear, with an estimated second-order rate constant of 7.4 ± 0.8 × 10^7 M^{-1} s^{-1}; at concentrations above 2 μM, the rate increases nonlinearly to an asymptotic value of approximately 300 s^{-1}, indicating the presence of a rate-limiting step in the process. The spectrum of the one-electron reduced enzyme suggests that Mo centers are largely reduced with a minor contribution of iron−sulfur cluster reduction. Under conditions favoring two-electron reduction of the enzyme, the redox difference spectrum can be accounted for by the oxidation of two reduced ferredoxins, suggesting that the enzyme has completed one full catalytic cycle. The spectral changes observed in the absence of nitrate are significantly different from those seen in the presence of nitrate. Experiments in the absence of nitrate revealed that the singly reduced enzyme exhibits different absorption characteristics and reoxidation kinetics, compared to those observed with nitrate present, and exhibits a much faster binding by reduced ferredoxin than the oxidized enzyme. The implications of these observations for understanding the enzyme mechanism are discussed.

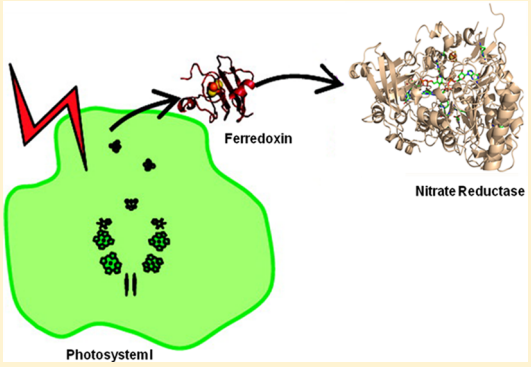

The pathway for nitrate assimilation in cyanobacteria includes three steps that involve redox chemistry.[1,2] The first of these is the two-electron reduction of nitrate to nitrite catalyzed by nitrate reductase (NR), which is followed by the nitrite reductase-catalyzed six-electron reduction of nitrite to ammonia. The ammonia reacts with glutamate, in a reaction catalyzed by glutamine synthetase, to form glutamine (glutamine formation involves ATP but does not involve any redox chemistry). In the final reaction of this portion of the pathway, glutamine reacts with 2-oxoglutarate, in the two-electron reduction catalyzed by glutamate synthase, to form two molecules of glutamate, in the final step of the reductive portion of the nitrate assimilation pathway.[1,2] In oxygenic photosynthetic eukaryotes, while ferredoxin (Fd) is the electron donor for both the reduction of nitrite to ammonia and of glutamine plus 2-oxoglutarate to glutamate, the reduction of nitrate to nitrite utilizes reduced pyridine nucleotide as the reductant.[1,2] However, in cyanobacteria, all three of the reductant-requiring steps utilize reduced ferredoxin (Fd_{red}) as the specific physiological electron donor.[1,2] As is also the case for nitrite reductases and glutamate synthases from several different species,[2] it has been demonstrated that the Fd-dependent NR from *Synechococcus* sp. PCC 7942 can form a 1:1 complex with Fd at low ionic strength.[3]

In many ways, the best characterized of the cyanobacterial Fd-dependent NRs is that from *Synechococcus* sp. PCC 7942 (the product of the *NarB* gene). This enzyme (hereafter abbreviated as NR) is a 78 kDa, soluble, monomeric enzyme that contains a single [4Fe-4S] cluster and a single Mo *bis*-molybdopterin guanine dinucleotide (MoMGD) center as its only prosthetic groups.[4,5] The oxidized $[4Fe\text{-}4S]^{2+}$ form of the iron−sulfur cluster is EPR silent, while one-electron reduction (E_m = −190 mV) produces a signal at 10 K characteristic of a $[4Fe\text{-}4S]^{1+}$ cluster.[5,6] Computer modeling[6] and the observation that the cluster is susceptible to oxidative damage that converts a portion of it to a [3Fe-4S] form[5,6] suggest that the cluster is situated in an exposed location in the protein. EPR spectra obtained at 60 K,[5,6] combined with redox poising, revealed a Mo(VI) to Mo(V) transition with E_m = −150 mV,[5] with most of the Mo(V) species displaying a "high *g*" EPR signal (g_{av} = 1.9897). Voltammetry measurements suggested that the nitrate

Received: March 29, 2014
Revised: July 18, 2014
Published: July 20, 2014

   dx.doi.org/10.1021/bi500386n | *Biochemistry* 2014, 53, 5092−5101

binds to the enzyme during the catalytic cycle when the enzyme is in a two-electron reduced state containing the MGD in the Mo(V) oxidation state and the [4Fe-4S]$^{1+}$ form of the cluster.[5]

An early site-directed mutagenesis study of *Synechococcus* sp. PCC 7942 NR identified Cys9, Cys12, Cys16, and Cys56 as likely ligands to the [4Fe-4S] cluster in *Synechococcus* sp. PCC 7942 NR.[4] A more recent site-directed mutagenesis study provided evidence for the importance of three basic amino acids in *Synechococcus* sp. PCC 7942, Lys58, Arg70, and Lys130, amino acids that are conserved in all Fd-dependent NR enzymes.[6] This study also produced an *in silico* model of the tertiary structure of *Synechococcus* sp. PCC 7942 NR (no crystal structure for the enzyme is currently available) that has provided useful insights into possible mechanism for the action of the enzyme.[6]

Despite this considerable body of knowledge about *Synechococcus* sp. PCC 7942 NR, nothing is known about the kinetics of electron transfer (hereafter abbreviated as ET) from reduced Fd to the enzyme, about the rates of internal ET, or about the kinetics of ET to the electron-accepting substrate, nitrate. We have thus undertaken a preliminary kinetic study of this cyanobacterial NR, using a flash photolysis technique in which reduced Fd is generated, using light activation of a cyanobacterial Photosystem I (PSI) reaction center (RC), and the rates of subsequent reactions involving the enzyme are monitored using absorbance transients in the visible and near-IR regions of the spectrum. This technique has previously proven useful for studying the mechanisms of other soluble Fd-dependent enzymes.[9−11]

MATERIALS AND METHODS

Biological Materials. All experiments were performed with PSI monomers from *Synechocystis* 6803[12] and a recombinant form of Fd from the same organism.[13] The PSI concentration was estimated by assuming a P700$^+$ absorption coefficient of 7.7 mM^{-1} cm^{-1} at 800 nm.[10] The Fd concentration was estimated by assuming an absorption coefficient of 9.7 mM^{-1} cm^{-1} at 422 nm.[11] Wild-type *Synechococcus* sp. PCC 7942 NR was expressed, purified, and characterized as described previously.[6] The Fd and NR samples used were 95% pure, as judged by SDS-PAGE.

Flash-Absorption Spectroscopy. Measurements were made as described previously.[10] The principle of the experiments is to generate reduced Fd, the physiological electron donor partner of NR,[4] by photoexcitation of PSI reaction centers.[11] A short laser flash is used which is saturating for PSI photochemistry (i.e., producing close to 100% primary charge separation, as monitored by the extent of P700 oxidation), by taking advantage of the very large PSI absorption cross section. The laser excitation (wavelength, 700 nm; duration, 6 ns; energy, 25 mJ) was provided by a dye (LDS 698, Exciton) laser (Sirah, Laser- and Plasmatechnik) pumped by a frequency-doubled Nd:YAG laser (Quanta-Ray, Spectra Physics).

After flash excitation, the terminal PSI electron acceptor is reduced in less than 1 μs. Then this acceptor reduces Fd in a multiphasic process with full Fd reduction completed in less than a few hundreds microseconds.[7] The amount of Fd_{red} formed after a flash is therefore equal to the concentration of PSI in which the terminal acceptor has been reduced. This part of PSI, which represents 97% of the total PSI concentration (the remaining 3% undergoes recombination processes with intrinsic PSI acceptors preceding the terminal one, as inferred from P700$^+$ decay in the microsecond to millisecond time range) is considered to be the active PSI, as it should be able to reduce Fd with high efficiency and at a high rate.[10] In the absence of NR, Fd_{red} is slowly reoxidized (i.e., in a few seconds) by dissolved oxygen, and the oxidized PSI primary electron donor (P700$^+$) is reduced over the same time period by an exogenous reductant, the reduced form of 2,6-dichlorophenolindophenol (DCPIP). The DCPIP, present at a concentration of 25 μM, is kept reduced by the presence of 2 mM sodium ascorbate in the reaction mixture. In this way the initial "resting" state of the RC is rapidly restored after a light flash, allowing signal averaging by repetitive flash excitation. The addition of NR, which is reduced by the Fd_{red} generated by the flash, results in a much more rapid reoxidation of the Fd_{red} (the conditions for recovery of the initial oxidized state of NR after a flash are described below in the Results section).

Three different wavelengths, 490, 580, and 800 nm, proved to be particularly useful during this study and thus have been used extensively during this work. The wavelength of 580 nm has been extensively used in previous papers studying Fd reduction by PSI[7,8] for technical reasons: significant absorption changes arising from Fd reduction by PSI occur at this wavelength; absorption by PSI itself is weak at this wavelength; and it is an isosbestic point for the formation of carotenoid triplets which may obscure the absorption signals in the μs time domain if a different wavelength were used. The wavelength of 490 nm has been chosen to study the time dependence of signal amplitude as a function of delay between consecutive flashes in the absence of nitrate, as the signal increase that results from an increased delay time between flashes was found to be much larger than was the case for observation at 580 nm. This choice was made after an initial exploratory examination of different wavelengths. The wavelength of 800 nm (or, more generally, a wavelength in the 800−830 nm range) is currently used in studies of PSI photochemistry for several reasons: first it corresponds to the maximum of P700$^+$ absorption in the near-infrared region; second it is not absorbed by chlorophyll or antenna pigments (including P700) so that it has no actinic effect and measuring light of large intensities can be used (hence a good signal-to-noise ratio); third, neither Fd nor any other PSI component (except P700$^+$), including its [4Fe-4S] clusters, makes any contribution to the absorption changes. Therefore, the kinetics of P700$^+$ formation and decay can be easily monitored at 800 nm. The P700$^+$ kinetics of Figure 2 were fitted with a monoexponential decay between 10 ms after the flash and 280 ms after the flash (the time point at the end of recording the signal) for traces a and b of Figure 2A ($t_{1/2}$ = 0.97 and 0.93 s, respectively) and for trace a of Figure 2B ($t_{1/2}$ = 1.01 s). Trace b of Figure 2B was fitted with the same function between 60 ms (end of decay attributed to NR) and 280 ms with a $t_{1/2}$ of 1.02 s (standard error of fits were 0.01−0.02 for all $t_{1/2}$). All experiments were carried out at a temperature of 295 K in reaction mixtures that contained, in addition to the 2 mM sodium ascorbate and 25 μM DCPIP mentioned above, 25 mM Tricine buffer (pH: 8.0), 30 mM NaCl, 5 mM $MgCl_2$, and 0.03% (W/W) *n*-dodecyl β-D-maltoside. The flash-induced absorption changes were always studied using two separate cuvettes containing exactly the same buffers, the same amounts of ascorbate and DCPIP, and exactly the same amounts of PSI and Fd. In the sample cuvette, NR was added as a small aliquot of a standard solution of the enzyme, and an equal volume of the same buffer was added to the reference cuvette. For reasons of stability, the buffer used for NR stock solution was 25 mM HEPES (pH 8.0) containing 100 mM NaCl. In some control

dx.doi.org/10.1021/bi500386n | *Biochemistry* 2014, 53, 5092−5101

experiments, a third cuvette containing PSI, but neither Fd nor NR, was used.[9] In another control experiment, two cuvettes were compared containing PSI with or without NR but no Fd. Samples were contained either in 1 cm square cuvettes or in 1 mm cuvettes which were placed at 45° angles to the measuring and exciting beams (resulting in an effective light path of 1.2 mm). A very similar approach has been previously used for studying two other partners of Fd, ferredoxin:NADP$^+$ oxidoreductase (hereafter abbreviated as FNR) and nitrite reductase.[10,11]

RESULTS

NR Reduction by Fd_{red} Depends upon the Presence of Nitrate. Figure 1 shows the flash-induced absorption changes

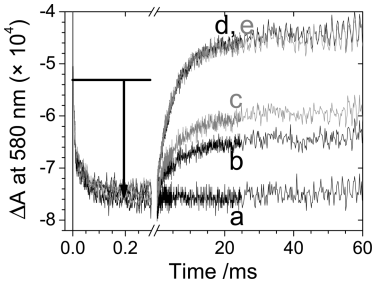

Figure 1. Electron transfer from Fd to NR: Dependence upon the presence of nitrate and the averaging conditions. Flash-induced absorption changes were measured at 580 nm in three different 1 cm cuvettes containing PSI/Fd (trace **a**), PSI/Fd/NR (traces **b** and **c**), PSI/Fd/NR/nitrate (traces **d** and **e**). The signals are shown with a breakpoint at 0.30−0.31 ms in order to show that all kinetics are almost indistinguishable at short times. Each trace represents the average of four measurements with either a 10 s (black traces **a**, **b**, and **d**) or a 2 min (gray traces **c** and **e**) delay between two consecutive measurements. Two (unrecorded) preflashes were given to the samples separated by either 10 s (**a**, **b**, and **d**) or 2 min (**c** and **e**). Traces **d** and **e** are almost indistinguishable. The drawn horizontal line corresponds to the signal level that was measured at short times on a sample containing only PSI so that the arrow corresponds to the bleaching associated with the fast reduction of Fd by PSI. Concentrations in 1 cm cuvettes: [PSI] = 0.25 μM; [Fd] = 2 μM; [NR] = 0 or 4 μM; [$NaNO_3$] = 0 or 1 mM.

at 580 nm due to ET from Fd_{red} to oxidized NR (NR_{ox}) in cuvettes containing PSI and Fd. This wavelength has been extensively used in previous papers studying Fd reduction by PSI.[7,8] In the control cuvette without NR (trace **a**), the absorbance decrease due to Fd reduction by the terminal PSI acceptor (indicated by a downward arrow) remains stable on a 60 ms time scale. This reflects the fact that the oxidation states of two species giving rise to absorption changes at times >300 μs, i.e., P700$^+$ and Fd_{red}, remain essentially unchanged on this time scale. In the presence of 4 μM NR (in excess over PSI and thus over Fd_{red} as well), the kinetics at short times after the flash (<300 μs) are almost identical to those observed in the absence of NR, and the absorption increase resulting from the presence of NR only becomes apparent at longer times (see the right panel of Figure 1, traces **b**−**e**). This absorption increase at 580 nm is attributed to reoxidation of Fd_{red} by NR_{ox} according to the reaction:

$$Fd_{red} + NR_{ox} \rightarrow Fd_{ox} + NR_{red1} \quad (1)$$

with NR_{red1} designating singly reduced NR. The signal size is much larger in the presence of nitrate (traces **d** and **e**) than in

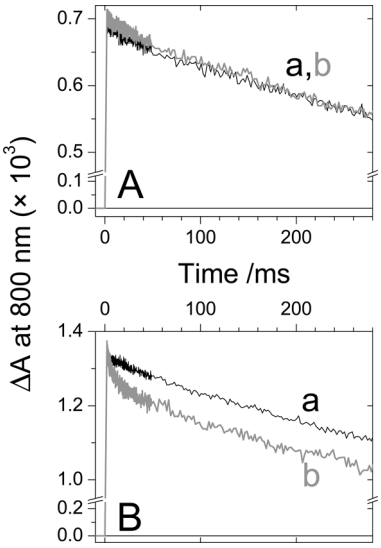

Figure 2. Flash-induced absorption changes at 800 nm reflecting mostly P700$^+$ formation and decay. These absorption changes were measured in two different 1 mm cuvettes (optical path length = 0.12 cm) either in the presence of 1 mM sodium nitrate (A) or in its absence (B). For both parts, traces **a** were measured with PSI and Fd, and traces **b** were measured with PSI, Fd, and NR. Traces **a** and **b** of (A) are almost superimposable. Traces **b** are shown in bold gray. Each trace represents the average of four measurements. (A): [PSI] = 0.75 μM, [Fd] = 8 μM, [NR] = 0 or 16 μM, [$NaNO_3$] = 1 mM. (B): [PSI] = 1.44 μM, [Fd] = 8 μM, [NR] = 0 or 16 μM. One measurement was made every 10 s except for trace **b** of (B), in which case one measurement was made every 3 min.

its absence (traces **b** and **c**). Moreover, in the absence of nitrate, the signal is smaller when the time interval between consecutive acquisitions is changed from 2 min (trace **c**) to 10 s (trace **b**). This time interval dependence is not observed in the presence of nitrate (trace **d** = trace **e**). These observations indicate that NR_{red1} returns to its initial NR_{ox} state much more rapidly in the presence of nitrate than in its absence. In a control experiment, it was shown that there is no direct ET from PSI to NR by demonstrating that the absorption changes obtained in a cuvette containing only PSI are superimposable with those obtained in a cuvette containing PSI and NR, with neither cuvette containing any Fd (data not shown).

Additional data (shown in Figures 3−6) that further characterize the differences between absorbance changes measured in the presence of NR and those measured in its absence (e.g., trace **d** *minus* trace **a** of Figure 1) are presented below. Using the differences between these absorbance changes eliminates contributions from Fd reduction by the PSI terminal electron acceptor, provided that PSI photochemistry and Fd reduction by PSI are not altered by the presence of NR. That these conditions are fulfilled is shown by the similarity in initial absorbance decays ±NR observed in Figure 1, which reflect these two processes. This subtraction procedure also eliminates absorption change contributions arising from changes in the redox state of the PSI primary donor, P700. The assumption that the subtraction procedure correctly eliminates changes arising from P700 can be tested by determining whether reduction of P700$^+$ is identical in the presence and absence of NR. That this is in fact the case is demonstrated in Figure 2, where P700 photo-oxidation and its subsequent decay in the dark period following the flash were monitored at 800 nm, i.e., at the near-infrared absorption maximum for P700$^+$.[10] One

dx.doi.org/10.1021/bi500386n | *Biochemistry* 2014, 53, 5092−5101

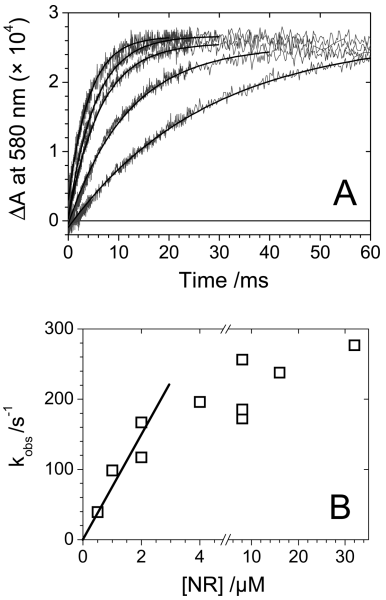

Figure 3. Electron transfer from Fd to NR in the presence of nitrate. Dependence upon the NR concentration. (A) Flash-induced absorption changes were measured at 580 nm in two different cuvettes containing PSI/Fd and PSI/Fd/NR mixtures. The representative traces correspond to the difference in signals between the second (+ NR) and the first (− NR) cuvettes, both containing 1 mM sodium nitrate. For the four kinetics with the slowest rises, the measurements were performed in 1 cm cuvettes containing 0.21 μM PSI, 2 μM Fd and NR concentrations of 0.5, 1, 2, and 4 μM (the rates of signal rise increase with the NR concentration). The fastest signal was measured with 1 mm cuvettes containing 1.36 μM PSI, 8 μM Fd, and 16 μM NR. This last signal was multiplied by a normalization factor of 1.3 corresponding to the ratio between the products ([PSI] × path length) for the two types of cuvette (0.21 μM × 1 cm =1.36 μM × 0.12 cm × 1.3). The data were fitted (black lines) with a single exponential rise $S(t) = a_0 + a_1 \times e^{-kt}$ with three free parameters a_0, a_1 and the rate k (a_1 being close to ($-a_0$) but not identical to account for the fact that the signal at short times may be not exactly zero). Each trace represents the average of four measurements (Δt = 10 s between two measurements). (B) The observed rates k of signal increase, as obtained from experiments similar to those of part A are plotted as a function of NR concentration. A linear fit (black line) was performed for NR concentrations up to 2 μM giving a slope of 7.4 ± 0.8 × 10^7 M^{-1} s^{-1}. Note that the standard errors of the exponential fits allowing the determinations of k_{obs} are of little size (and therefore are not shown) compared to data scattering. We have no good explanation for this data scattering.

advantage of using absorption at 800 nm to monitor $P700^+$ is that there are no absorption contributions from Fd or from P700 or any other PSI component at this wavelength. The fast initial signal rise results from P700 photo-oxidation, and the subsequent slow signal decay is caused by the reduction of $P700^+$ by exogenous $DCPIPH_2$. In the presence of nitrate this signal decay is similar whether NR is present or absent (Figure 2A). The situation is different in the absence of nitrate (Figure 2B), where the signal with NR exhibits a faster initial decay (trace **b** vs trace **a**) before both signals decay slowly in parallel (see data fits of slow decays in Materials and Methods). The slow decay observed in the absence of nitrate, which does not depend upon NR, can be attributed to $P700^+$ reduction alone, as is the case in the presence of nitrate, while NR contributes to the absorption changes observed at shorter times (<20 ms).

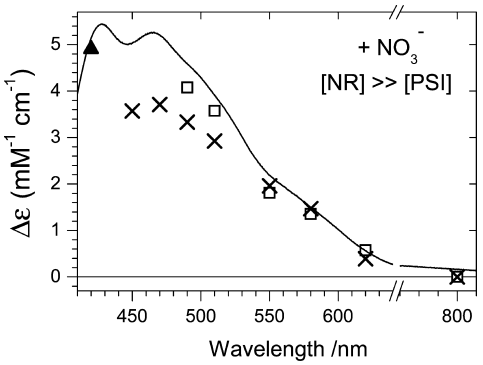

Figure 4. Spectrum of NR reduction by Fd_{red} in the presence of nitrate, with NR in large excess over PSI. The data were obtained from differences in absorption changes, as shown for the two fastest kinetics at 580 nm in Figure 3, by taking the amplitudes after completion of the signal rise (a signal increase being plotted as a positive amplitude, average of four measurements for each data point; data fitted with a constant between 25 and 40 ms after the flash). Three different data sets are mixed together in this figure with different PSI, Fd, and NR concentrations. First set with 1 cm cuvettes: [PSI] = 0.2 μM, [Fd] = 2 μM, [NR] = 2 μM; measurements above 490 nm (data are plotted as open squares). Second set with 1 cm cuvettes for measurement at 420 nm, where PSI absorption is large: [PSI] = 0.05 μM, [Fd] = 2 μM, [NR] = 2 μM (data indicated by a filled-in triangle). For these two sets of measurements, one measurement was made every 10 s. The third set (with the data plotted as crosses) was obtained using 1 mm cuvettes (crosses) and [PSI] = 0.75 μM, [Fd] = 8 μM, [NR] = 16 μM, with one measurement every 7 s. Note that the standard error of the fit parameter (<0.03 mM^{-1} cm^{-1}) is of small size (and therefore is not shown) compared to the difference between signals measured under two different conditions (square and cross at a single wavelength). The vertical scale was converted to millimolar absorption coefficients from the PSI concentration. The continuous line corresponds to the Fd difference spectrum (Fd_{ox} − Fd_{red}).

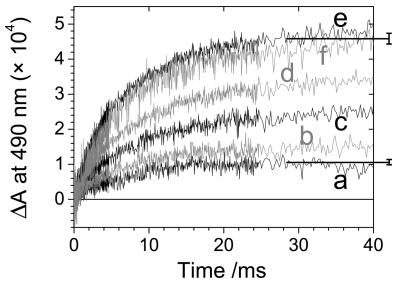

Figure 5. Electron transfer from Fd to NR in the absence of nitrate. Dependence upon the time delay between consecutive measurements. Flash-induced absorption changes were measured at 490 nm in two different 1 mm cuvettes containing PSI/Fd and PSI/Fd/NR mixtures in the absence of nitrate. The traces correspond to the difference in signals between the second (+ NR) and the first (− NR) cuvettes. Each trace was obtained after giving two (unrecorded) preflashes to the sample. Time intervals between the unrecorded preflashes and the single measurement (no averaging) were the same. Traces **a**–**f** correspond to time intervals of 10 s, 30 s, 1, 2, 3, and 5 min. [PSI] = 1.50 μM; [Fd] = 8 μM; [NR] (when present) = 16 μM. The horizontal lines (and standard errors) correspond to another experiment (see text) with alternating Δt values of 3 min (upper line) and 10 s (lower line). [PSI] = 1.50 μM; [Fd] = 8 μM; [NR] (when present) = 16 μM.

NR Reduction by Fd_{red} in the Presence of Nitrate. The kinetics of NR reduction by Fd_{red} in the presence of nitrate were studied at different NR concentrations, in all cases with

dx.doi.org/10.1021/bi500386n | *Biochemistry* 2014, 53, 5092−5101

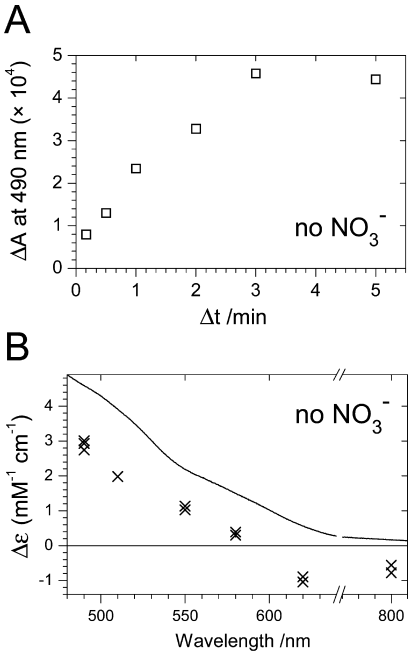

Figure 6. NR reduction by Fd_{red} in the absence of nitrate.Spectrum and dependence upon the delay time between two consecutive flashes. The signals were obtained after fitting the data with a constant between 35 and 45 ms after the flash. (A) Signal size dependence upon the delay time between two consecutive measurements (obtained from Figure 5). For each data point, the standard error of the fit (0.03 to 0.04 × 10^{-4}) is 4–6 times less than the noise level of each measurement (0.12 to 0.19 × 10^{-4}). (B) Spectrum of NR reduction by Fd_{red} with NR in large excess over PSI. The measurements (three at 490 nm, one at 510 nm, two at other wavelengths) were made under low repetition rate conditions: using a 3 min delay, two preflashes were given, and then one signal was recorded (no averaging). Two different samples were studied. Note that the standard error of the fit parameter (<0.04 mM^{-1} cm^{-1}) is of small size (and therefore is not shown) compared to data scattering from different measurements at a given wavelength. The vertical scale was converted to millimolar absorption coefficients from the PSI concentration. The continuous line corresponds to the Fd difference spectrum (Fd_{ox} − Fd_{red}).

NR in excess over PSI ([PSI] = [Fd_{red}] at short times) so that transfer of a single electron to NR, according to Reaction 1 is favored over the transfer of two electrons to the enzyme. The kinetics of this reaction, monitored using the differences between signals with and without NR, are shown in Figure 3A. The reaction rate increases with increasing [NR] and the observed kinetic data are well fitted by a monoexponential rise (continuous lines). The rates derived from these fits were plotted as a function of [NR] in Figure 3B. Two regions can be distinguished in this plot. At low concentrations (≤2 μM), the concentration dependence is approximately linear, whereas at high concentrations, the rate increases more slowly to an asymptotic value of about 300 s^{-1}. Fitting the linear part allows a second-order rate constant of 7.4 ± 0.8 × 10^7 M^{-1} s^{-1} to be estimated for NR_{ox} reduction (Reaction 1). The asymptotic behavior reveals the involvement of a rate-limiting reaction during NR_{ox} reduction and indicates that Reaction 1 is not sufficient to describe the reduction process at high NR concentrations. The transition region between the linear and asymptotic regions i.e., where the rate does not increase linearly with increasing [NR] but still depends upon [NR], occurs between 2 μM and 10 μM. One would expect that the contribution of first-order, intracomplex electron transport would be increasing over this concentration range. Although these concentrations are below the value of 38 μM reported for the K_M value for Fd,[6] it is possible that the K_d for the dissociation of Fd_{red} from NR_{ox} lies in this range. It should also be noted that one can also conclude, from the amplitudes of the signals in Figure 3A, that the reverse of Reaction 1 occurs to a negligible extent. If this were not the case, the final signal amplitude would increase with the NR concentration, something that clearly does not occur.

The spectrum for single reduction of NR (products *minus* reactants of Reaction 1), obtained from kinetic traces similar to those of Figure 3 under conditions where NR is in large excess over PSI, is shown in Figure 4. The vertical scale was converted to millimolar absorption coefficients from the concentration of "active" PSI (PSI where the terminal acceptors are reduced after a flash, as described in Materials and Methods). As all these PSI reaction centers will reduce Fd[8] and as Reaction 1 is quasi-irreversible under these experimental conditions, comparing the experimental spectrum to the spectrum of (Fd_{ox} − Fd_{red}) (continuous line) should reveal the NR contribution. The difference between the two spectra thus indicates that a one-electron reduction of NR in the presence of nitrate results in an absorption decrease in the region from 450 to 550 nm and to little or no change outside this region.

Reduction of NR by Fd_{red} was also studied at a PSI concentration twice that of NR (and with Fd in large excess over the two other proteins). Under these conditions, it is expected that a significant portion of the NR present will accept two electrons from two consecutive interactions with a Fd_{red} and undergo a full catalytic cycle, converting nitrate to nitrite. As NR should return to its oxidized state at the end of the cycle, the spectrum of the absorption changes during a cycle should correspond to those expected only for oxidation of two Fd_{red} to two Fd_{ox}. As shown in Figure SI.1 in the Supporting Information (SI), the data come close to meeting this prediction, with the observed spectrum closely approximating that expected for the oxidation of 1.70 Fd_{red} (i.e., 85% of the difference spectrum expected for the oxidation of two Fd_{red}, with no contributions from additional components).

NR Reduction by Fd_{red} in the Absence of Nitrate. Data shown in Figure 1 indicate that, in the absence of nitrate, the absorption change associated with Reaction 1 depends upon the time interval, Δ*t*, between the consecutive measurements that were used for signal averaging, suggesting that NR_{red1} is reoxidized slowly under these conditions. We explored this phenomenon more systematically by studying the signal elicited by the third flash following two unrecorded preflashes, with all flashes being separated by the same time interval. This dependence on Δ*t* is shown in Figure 5 for signals measured at 490 nm with Δ*t* varying from 10 s to 5 min. The signal amplitude increases up to a Δ*t* of 3 min and no significant change is observed between 3 and 5 min, as also shown in Figure 6A. A qualitatively similar experiment was performed at 580 nm. However, in this case, the increase of signal size with Δ*t* is much smaller (see traces b and c in Figure 1 and compare spectra in Figure 6B and Figure SI.3 in the SI) so that the Δ*t* dependence determined at this wavelength is much less precise than is the case based on measurements made at 490 nm. Two points about the results of this experiment are worth emphasizing: (1) In the presence of nitrate, the shortest Δ*t* that was tested (10 s) gives the maximum signal amplitude with no increase at larger Δ*t* (data not shown), in line with data of Figure 1. (2) These observations were made with a large excess

dx.doi.org/10.1021/bi500386n | *Biochemistry* 2014, 53, 5092–5101

of NR over PSI (i.e., at a ratio >10), conditions that make it impossible for a reduced NR species to accumulate in excess over NR_{ox} during the two preflashes. In another experiment, every flash-induced signal was recorded in a series of flashes with alternating Δt values of 3 min for odd-numbered flashes (first, third, fifth, ... up to the 11th flash) and 10 s for even-numbered flashes (second, fourth, sixth,... up to the 12th flash). In this experiment, each individual signal was similar to that shown in trace **e** (odd flash number), or in trace **a** (even flash number) of Figure 5 (black horizontal lines). This shows unambiguously that the difference in signal size cannot be attributed to the accumulation of a reduced NR species.

As stated above, Reaction 1 appears to be almost irreversible in the presence of nitrate over the range of protein concentrations used. This is also shown in Figure SI.2B in the SI, together with an experiment made at very similar protein concentrations, but without nitrate (Figure SI.2A in the SI) and at large Δt. In the latter case, the signal size increases with [NR] (>[PSI]), which suggests that ET is incomplete at the lowest NR concentration that was tested (0.5 μM vs 0.19 μM PSI). The equilibrium constant for Reaction 1 (in its reversible form) can be calculated, in principle, from this type of experiment. However, further work is needed before such a calculation can be made reliably for the following reasons: (1) The Δt dependence of the signal amplitude must be carefully evaluated, as the presence of residual NR_{red1} may have a strong influence on the signal size when [NR] is small. (2) These experiments should be repeated at several [NR], as we plan to do in future studies. Nevertheless, our results suggest that the midpoint potential for the one-electron reduction of NR_{ox} is much more negative in the absence of nitrate than in its presence. From our data, we estimate that $E_m(NR_{\text{first reduction, no nitrate}})$ is probably lower than −300 mV (see the legend of Figure SI.2A in the SI). This appears to be in contradiction to the determination of NR midpoint potentials reported by Jepson et al.,[5] i.e., E_m ($[4Fe\text{-}4S]^{2+}$/ $[4Fe\text{-}4S]^{1+}$= −190 mV; E_m (Mo^{6+}/Mo^{5+}) = −150 mV, both of which were measured in the absence of nitrate. A tentative interpretation of this result will be given in the Discussion.

The spectra of NR reduction by Fd_{red} were measured in the absence of nitrate and with a large excess of NR over PSI both with a 10 s (Figure SI.3 in the SI) and a 3 min delay (Figure 6B) for NR_{red1} reoxidation (hereafter referred to as the 10 s and 3 min spectra). The 3 min spectrum observed in the absence of nitrate differs significantly from that observed in the presence of nitrate (Figure 4), as can be seen by the smaller amplitude of the positive signal at 580 nm and by the negative signals observed at 620 and 800 nm. The signal observed after a short Δt (traces **a** and **b** in Figure 5 for Δt = 10 and 30 s, respectively) can be used to estimate a lower limit for the rate constant for the association of Fd_{red} with NR_{red1}. Under the conditions used for the experiments of Figure 5, NR_{ox} reduction by 100% of photoreduced Fd_{red} should give a signal of 5.2×10^{-4} ($\Delta\varepsilon \times [Fd_{red}] \times$ light path, with $\Delta\varepsilon$ = 2900 M^{-1} cm^{-1} from Figure 6B, $[Fd_{red}]$ = [PSI] = 1.50 μM, light path = 0.12 cm), which is approximately 5 times larger than what is observed for trace **a**. We can therefore hypothesize that the rate of association of Fd_{red} with NR_{red1} is about 5 times larger than the rate of NR_{ox} reduction (~270 s^{-1} under the present conditions; see Figure 3B). Thus, $k_{observed} \approx k_2 \times [Fd_{red}] = 270 \times 5 \approx 1350$ s^{-1} which gives, with $[Fd_{red}]$ = 1.5 μM, $k_2 \approx 9 \times 10^8$ M^{-1} s^{-1}. This value is quite high, but even larger values have been previously found for protein−protein association involving Fd.[14] One can note, however, that this rate calculation should be viewed with considerable caution as the specific recognition of NR_{red1} by Fd_{red} should lead to double reduction of NR, and the absorption changes associated with that process may contribute in a way that will affect the above estimate.

DISCUSSION

Single NR Reduction in the Presence of Nitrate Probably Involves Reduction of the Mo Atom. The kinetics of single NR reduction by Fd_{red} are much simpler to study in the presence than in the absence of nitrate, because flash excitation can be used for signal averaging (using a Δt between flashes ranging from 7 to 10 s) without any detectable change in either signal amplitude or shape. This is most probably due to NR_{red1} reoxidation during the time interval between two consecutive flashes. For this reason our characterization of the kinetics of the one-electron reduction of NR by Fd_{red} in the presence of nitrate is more extensive and more detailed than was the case for the kinetics observed in the absence of the electron-accepting substrate of the enzyme. The second-order rate constant measured for this reaction, $7.4 \pm 0.8 \times 10^7$ M^{-1} s^{-1}, is 3−7 times smaller than the rate constant that was previously measured with two other Fd partners, FNR and nitrite reductase.[10,11] A maximal value of 300 s^{-1} was observed at high NR concentrations, indicating the involvement of a rate-limiting step. From the known structures of enzymes related to the *Synechococcus* sp. PCC 7942 NR used in this study and our previously published *in silico* model for the *Synechococcus* sp. PCC 7942 enzyme,[6] it is very likely that within the Fd−NR complex, single ET occurs from Fd to the [4Fe-4S] cluster of NR and then from the NR cluster to the Mo atom, according to the following scheme of reactions (primed numbers are used to differentiate these reactions from Reaction 1 defined above whereas X and: (colon) are used to designate complexes between the two proteins):

$$Fd_{red} + NR_{ox} \leftrightarrow Fd_{red}X\,NR_{ox} \quad (1')$$

$$Fd_{red}X\,NR_{ox} \leftrightarrow Fd_{red}{:}\,NR_{ox} \quad (2')$$

$$Fd_{red}{:}\,([4Fe-4S]^{2+}Mo^{6+}) \leftrightarrow Fd_{ox}{:}\,([4Fe-4S]^{1+}Mo^{6+}) \quad (3')$$

$$Fd_{ox}{:}\,([4Fe-4S]^{1+}Mo^{6+}) \leftrightarrow Fd_{ox}{:}\,([4Fe-4S]^{2+}Mo^{5+}) \quad (4')$$

$$Fd_{ox}{:}\,NR_{red1} \leftrightarrow Fd_{ox} + NR_{red1} \quad (5')$$

with both NR cofactors being oxidized in Reactions 1′ and 2′ (NR_{ox} = $[4Fe\text{-}4S]^{2+}$ − Mo^{6+}; X in the right term of 1′ and left term of 2′ indicating that no, or very slow, ET can occur within the complex; : (colon) in the right term of 2′, in both terms of 3′ and 4′ and in the left term of 5′ indicating that the complex is competent for ET) and NR_{red1} being singly reduced NR. For the sake of simplicity, complex dissociation after ET was described by a single reaction despite the fact that, in principle, NR_{red1} could correspond to two distinct chemical species (one with Mo being reduced and the other with the iron−sulfur cluster being reduced). In this scheme, we assume that the initial complex formation, Reaction 1′, leads to an unproductive complex (i.e., one in which there is no reoxidation of Fd_{red} by NR) so that Reaction 2′ corresponds to the subsequent formation of a productive complex from the unproductive one.

dx.doi.org/10.1021/bi500386n | *Biochemistry* 2014, 53, 5092−5101

Such an interprotein gating process has been previously proposed in the case of the interaction between Fd and FNR[15] and has been found in many other systems.[16] According to this scheme, the second-order rate that we derived from the linear dependence of k_{obs} vs [NR] (Figure 3B) may not be a true rate constant if the initial binding of Fd_{red} to NR_{ox} leads to an unproductive complex, and consequently, it should be considered as a minimum value (the rate constant of complex formation in Reaction 1 may be larger than the apparent one that we are measuring).

The asymptotic rate that is measured at high [NR] (300 s^{-1}) may involve one or several rate-limiting steps in the above scheme. It could involve the forward Reactions in 2′, 3′ or 4′. It appears unlikely that Reaction 4′ is rate limiting as this would lead to the transient accumulation of a reduced [4Fe-4S] cluster (before its reoxidation by Mo^{6+}). Not only did we not observe any intermediate state while monitoring the kinetics of absorbance changes, but accumulation of NR with a reduced [4Fe-4S] cluster would have resulted in an absorbance decrease at wavelengths below 450 nm—something that was not observed. This reasoning assumes that the oxidized and reduced forms of the [4Fe-4S] cluster of NR have absorption properties typical of such clusters—in particular that $\Delta\varepsilon_{ox\text{-}red}$ at 420−440 nm is approximately 8 mM^{-1} cm^{-1},[17] a value that is significantly larger than the value of 5 mM^{-1} cm^{-1} measured for the [2Fe-2S] cluster in Fd.[10] It has previously been reported that the reduction of *Synechococcus* sp. PCC 7942 NR results in a very large bleaching ($\Delta\varepsilon \approx 20-25$ mM^{-1} cm^{-1}) in the region from 400 to 600 nm, a bleaching that was attributed largely to reduction of the enzyme's iron−sulfur cluster.[5] However, it should be emphasized that this extremely large bleaching is not at all typical of that observed for a [4Fe-4S] cluster. It is very unlikely that this discrepancy can be attributed to a major contribution arising from a change in the oxidation state of Mo, as these changes typically give difference spectra with $\Delta\varepsilon < 2$ mM^{-1} cm^{-1} (see below). Moreover, the reduction of such a cluster is generally associated with a weak bleaching above 600 nm,[18−21] in contrast to what can be seen in Figure 1A of Jepson et al.[5] In summary, we propose that the forward reaction in 4′ is not rate-limiting, in agreement with the hypothesis that the one-electron reduction of NR involves only a transient reduction of the [4Fe-4S] cluster, followed by the fast reduction of Mo with the concomitant reoxidation of the reduced cluster.[5]

One can estimate a rate for ET from the reduced [4Fe-4S] to Mo using Marcus theory[22] if one knows the distance between the electron donor and acceptor. A value of 12.2 Å for this distance can be estimated from our *in silico* model for the enzyme,[6] but a better defined distance of 8.5 Å between the closest sulfur atoms from a cysteine ligand to the cluster and the closest MGD ligand to the Mo can be calculated from the published crystal structure of a related enzyme, i.e., the periplasmic nitrate reductase from *Desulfovibrio desulfuricans*.[23] Using the latter distance and the least favorable values for the other Marcus parameters (i.e., zero for ΔG and 1.4 eV for the reorganization energy, λ) a rate of 5.2×10^5 s^{-1} can be calculated from eq 1 of ref 22. This estimated rate is consistent with our hypothesis that reduction of the Mo by the reduced [4F-4S] cluster is sufficiently rapid so that one would not expect an intermediate form of NR, in which the cluster is reduced but the Mo is still oxidized, to accumulate to a significant extent under the conditions of our kinetic measurements.

Additional studies (e.g., employing mutated Fd variants with modified midpoint potentials and/or mutated NR variants with modified affinities for Fd) are required to determine whether Reaction 2′ or 3′. i.e., forward rates of productive complex formation or reoxidation of Fd_{red}, respectively, are rate-limiting. One can also note that, in the framework of the above model, the rate of ET within the productive complex Reaction 3′ may be greater than 300 s^{-1} if Reaction 2′ is either rate-limiting or corresponds to an equilibrium with a significant population of nonproductive complex.

One can conclude from the spectrum shown in Figure 4 that NR reduction should contribute to an absorption decrease observed between 450 and 550 nm. Two interpretations, which are not mutually incompatible, for this observation are possible. (1) Reaction 4′ may not be complete and, as a result, the electron donated to NR by Fd_{red} is distributed between the [4Fe-4S] cluster and Mo. In fact, such a distribution, as opposed to a situation in which ET to the Mo is complete, would be expected from the report that the midpoint potential for the NR Mo(VI)/Mo(V) redox couple is only 40 mV higher than that of the iron−sulfur cluster.[5] If these E_m values, which were measured in the absence of nitrate,[5] are also true in the presence of nitrate (i.e., under the conditions used for the experiment of Figure 4), one can calculate that ∼18% of cluster will remain reduced at redox equilibrium in singly reduced NR. (2) A second possible interpretation of the absorption decrease may be due, at least in part, to reduction of Mo(VI) to Mo(V). There is relatively little information available in the literature about changes, arising from Mo reduction, in the UV−visible spectra of bis-molybdopterin enzymes. The data are in fact limited to measurements made with DMSO reductases from two *Rhodobacter* species (i.e., *R. sphaeroides* and *R. capsulatus*).[24−27] In these investigations, using enzymes that do not contain any prosthetic group other than the bis-molybdopterin cofactor, Mo(VI) was generally found to exhibit a weak absorption above 400 nm ($\varepsilon < 2$ mM^{-1} cm^{-1}) and its reduction, possibly to Mo(IV) but most probably to Mo(V),[26] has been reported to be accompanied either by an absorption decrease across the entire visible region,[24,25,27] or by absorption decreases above 600 nm and a small absorption increase in the region between 480 and 600 nm.[26] Clearly, a more detailed reduced *minus* oxidized spectrum associated with one-electron reduction of NR, along with additional information about the electron distribution between cofactors in this state (perhaps obtainable from future EPR experiments), will be required before a definitive choice between these explanations will be possible.

Fast Binding of Fd_{red} on Singly Reduced NR in the Absence of Nitrate May Provide Insight into the Catalytic Mechanism. A particularly intriguing phenomenon observed during our study is that after single reduction of only a small proportion of NR by Fd_{red} in the absence of nitrate (NR being in large excess over PSI), a second flash gives much smaller absorption changes when it is delivered a short time after the first one. This observation has two important implications. First, the state which is produced by the first flash (hereafter named NR_{red1b}, in order to distinguish it from NR_{red1} in the presence of nitrate) is highly stable, with its complete disappearance requiring a few minutes (Figures 5 and 6A); second, this state is recognized much faster by Fd_{red} than is the case for NR_{ox}. If this were not the case, the second flash should give a signal very similar in amplitude to that of the first flash, as NR_{ox} is in large excess over NR_{red1b}.

Our measurements also revealed a discrepancy between the incomplete ET between Fd_{red} and NR_{ox} in the absence of nitrate and what would be predicted on the basis of the E_m values previously reported[5] for the two prosthetic groups of the same NR used in the current study. It seems reasonable to assume that this is due to an effect of Fd binding, with a strong decrease in the ET equilibrium constant (for NR reduction) in the bound vs the free/unbound state. In such a case, consideration of the requirements of a thermodynamic cycle would lead one to conclude that the dissociation constant K_d after ET (i.e., Reaction 5′) is larger than its value before ET. In this context, it becomes necessary to reconcile an unfavorable association of Fd_{ox} and NR_{red1b} with a specific and (probably) fast recognition of NR_{red1b} by Fd_{red}. It is clear that a substantial amount of additional evidence must be gathered to substantiate the possibility that protein−protein recognition depends on the redox states of Fd and NR in this system.

A comparison of the spectrum obtained in the presence of nitrate with that obtained in its absence (Figures 4 and 6B) clearly shows that NR_{red1} and NR_{red1b} are different states (note, for example, that reduction of NR_{ox} to NR_{red1b} leads to absorbance decreases at 620 and 800 nm, unlike what is observed for NR_{red1}). As discussed above, reduction of [4Fe-4S] clusters generally leads to small absorbance decreases above 600 nm, and furthermore these decreases are smaller than those due to Fd reduction. Reduction of a [4Fe-4S] cluster by Fd is therefore expected to lead to an absorbance increase at 620 nm and to almost no change at 800 nm (both types of clusters giving very little, if any, change, at this wavelength. See for example ref 21.). Therefore, we attribute the signal decreases at 620 and 800 nm to reduction of the molybdenum. Of course, in principle, it could be argued that the [4Fe-4S] cluster in NR has highly unusual absorption properties. This seems unlikely, for the following reasons: (1) The EPR spectra of the reduced cluster in the wild-type enzyme are quite typical of those expected for a reduced [4Fe-4S] cluster;[5,6] and (2) it would also be necessary to postulate that the cluster is peculiar in the absence of nitrate but not in its presence, given that no absorbance decrease at 620 and 800 nm was observed in the presence of nitrate. It seems difficult to justify this additional assumption. Therefore, it seems likely that most of Mo is reduced (presumably from VI to V), both in the presence and absence of nitrate, but that changes in the coordination sphere and/or in the local microenvironment of the Mo lead to differences in absorption properties.

The spectra ± nitrate (Figures 4 and 6B) also differ below 600 nm, as a smaller signal amplitude is observed without nitrate, which points to a larger contribution (absorbance decrease) of NR. As discussed above for the spectrum measured in the presence of nitrate, a portion of this absorbance decrease may be due to the fact that the [4Fe-4S] cluster is in fast redox equilibrium with Mo and remains partially reduced because of the relatively small difference in the E_m values of the two prosthetic groups. The fact that this decrease is larger without nitrate could be due either to a larger contribution of cluster reduction arising from a smaller equilibrium constant for Reaction 4′ in the absence of nitrate than in its presence, or to a larger contribution of Mo reduction caused by a substrate-induced change in the intrinsic absorption properties of the Mo.

As discussed above, our results suggest that NR_{red1b} and NR_{ox} differ significantly in affinity and in binding kinetics for Fd_{red}. Presumably these differences would result from a conformational change in the enzyme, resulting from its reduction. The rate of this binding process is difficult to estimate, as we cannot completely exclude the possibility that the small absorbance changes observed under these conditions (see trace **a** in Figure 5 and the spectrum in Figure SI.3 in the SI) are not arising from a low efficiency of NR_{ox} reduction. The fact that Fd_{red} binding to NR_{red1b} results in only small absorption changes may be due to either an inhibition of ET or to reduction of the [4Fe-4S] cluster of NR by Fd_{red}.

Both of the characteristics of NR_{red1b}, described above (i.e., its relative stability (compared to NR_{red1}) and its preferential recognition by Fd_{red} (compared to NR_{ox})) would be expected to increase the catalytic efficiency of NR. The two effects, both individually and in combination, would favor double NR reduction when the enzyme does not have nitrate bound at the active site. This would eventually lead to the rapid 2-electron formation of nitrite once nitrate binding has occurred. An explanation for why this appears not to be the case in the presence of nitrate will require additional experimental data, and obtaining such data is a goal of our continuing kinetic investigation of the enzyme.

CONCLUSION

At the current time, there is no clear consensus on many aspects of the mechanism of Mo-containing enzymes that catalyze the two-electron reduction of nitrate to nitrite. For example, there has been disagreement about whether nitrate binding to reduced Mo involves the (IV) oxidation state of Mo (see, for example, ref 28) or the (V) oxidation state (see, for example, ref 5). Moreover, although it was generally accepted that nitrate binds directly to Mo, the possibility of initial binding to the second coordination sphere has recently received some support.[23] It has been also proposed that nitrate reduction to nitrite involves an oxidation of sulfur rather than of Mo.[29] Our results provide evidence for differences in the coordination sphere of Mo whether nitrate is present or not. Our future research will focus on providing more detailed information about the state of Mo in different states of the enzyme along with the further characterization of singly reduced NR in the absence of nitrate (a species which we found to be relatively long-lived). This may help in selecting between different possible mechanisms of the NR catalytic cycle.

ASSOCIATED CONTENT

Supporting Information

Three figures and their accompanying figure legends. This material is available free of charge via the Internet at http://pubs.acs.org.

AUTHOR INFORMATION

Corresponding Author

*Telephone: 806 834 6892. Fax: 806-742-1289. E-mail: david.knaff@ttu.edu.

Funding

The protein expression and purification, plus some aspects of the experimental design, data analysis and interpretation, carried out at Texas Tech University were funded by the Division of Chemical Sciences, Geosciences, and Biosciences, Office of Basic Energy Sciences of the U.S. Department of Energy, through Grant DE-FG03-99ER20346 (to D.B.K.). The flash photolysis experiments were carried out in the laboratory

of P.S. at CEA Saclay. A.P.S. was supported in part, by a scholarship from the Texas Tech University Graduate School. P.S. was supported, in part, by the French Infrastructure for Integrated Structural Biology (FRISBI) ANR-10-INSB-05-01.

Notes

The authors declare no competing financial interest.

■ ACKNOWLEDGMENTS

The authors would like to thank Prof. Luis Rubio and Prof. Enrique Flores for the gift of the clone used to express the *Synechococcus* sp. PCC 7942 NR and for their advice. The authors would also like to thank Prof. James P. Allen for calculating the distance between the two prosthetic groups in the *in silico* model of NR. The authors would also like to thank Dr. Bernard Lagoutte for purification of PSI and Fd and Ms. Véronique Mary for her expert technical assistance.

■ ABBREVIATIONS:

DCPIP, 2,6-dichlorophenolindophenol; $DCPIPH_2$, reduced DCPIP; EPR, electron paramagnetic resonance; ET, electron transfer; FNR, ferredoxin:$NADP^+$ oxidoreductase; Fd, ferredoxin; Fd_{red}, reduced ferredoxin; HEPES, 4-(2-hydroxyethyl)-1-piperazine ethanesulfonic acid; MALDI-TOF, matrix-assisted laser desorption ionization, time-of-flight; MGD, molybdopterin guanine dinucleotide; NR, nitrate reductase; NR_{ox} and NR_{red1}, oxidized and singly reduced NR; RC, reaction center; SDS-PAGE, polyacrylamide gel electrophoresis in the presence of sodium dodecyl sulfate

■ REFERENCES

(1) Hase, T., Schürmann, P., and Knaff, D. B. (2006) The interaction of ferredoxin with ferredoxin-dependent enzymes, in *Photosystem 1* (Golbeck, J. H., Ed.) pp 477−498, Springer, Dordrecht.

(2) Suzuki, A., and Knaff, D. B. (2005) Nitrogen metabolism and roles of glutamate synthase in higher plants. *Photosynth. Res. 83*, 191−217.

(3) Hirasawa, M., Rubio, L. M., Griffin, J. L., Flores, E., Herrero, A., Li, J., Kim, S.-K., Hurley, J. K., Tollin, G., and Knaff, D. B. (2004) Complex formation between ferredoxin and *Synechococcus* ferredoxin:nitrate oxidoreductase. *Biochim. Biophys. Acta 1608*, 155−162.

(4) Rubio, L. M., Flores, E., and Herrero, A. (2002) Purification, cofactor analysis, and site-directed mutagenesis of *Synechococcus* ferredoxin-nitrate reductase. *Photosynth. Res. 72*, 13−26.

(5) Jepson, B. J. N., Anderson, L. J., Rubio, L. M., Taylor, C. J., Butler, C. S., Flores, E., Herrero, A., Burt, J. N., and Richardson, D. J. (2004) Tuning a nitrate reductase for function. The first spectropotentiometric characterization of a bacterial assimilatory nitrate reductase reveals novel redox properties. *J. Biol. Chem. 279*, 32212−32218.

(6) Srivastava, A. P., Hirasawa, M., Bhalla, M., Chung, J.-S., Allen, J. P., Johnson, M. K., Tripathy, J. N., Rubio, L. M., Vaccaro, B., Subramanian, S., Flores, E., Zabet-Moghaddam, M., Stitle, K., and Knaff, D. B. (2013) The roles of four conserved basic amino acids in a ferredoxin-dependent cyanobacterial nitrate reductase. *Biochemistry 52*, 4343−4353.

(7) Sétif, P., and Bottin, H. (1994) Laser flash absorption spectroscopy study of ferredoxin reduction by photosystem I in *Synechocystis* sp. PCC 6803: Evidence for submicrosecond and microsecond kinetics. *Biochemistry 33*, 8495−8504.

(8) Sétif, P., and Bottin, H. (1995) Laser flash absorption spectroscopy study of ferredoxin reduction by photosystem I: Spectral and kinetic evidence for the existence of several photosystem I-ferredoxin complexes. *Biochemistry 34*, 9059−9070.

(9) Kuznetsova, S., Knaff, D. B., Hirasawa, M., Lagoutte, B., and Sétif, P. (2004) Mechanism of spinach chloroplast ferredoxin-dependent nitrite reductase: Spectroscopic evidence for intermediate states. *Biochemistry 43*, 510−517.

(10) Cassan, N., Lagoutte, B., and Sétif, P. (2005) Ferredoxin-$NADP^+$ reductase. Kinetics of electron transfer, transient intermediates, and catalytic activities studied by flash-absorption spectroscopy with isolated photosystem I and ferredoxin. *J. Biol. Chem. 280*, 25960−25972.

(11) Sétif, P., Hirasawa, M., Cassan, N., Lagoutte, B., Tripathy, J. N., and Knaff, D. B. (2009) New insights into the catalytic cycle of plant nitrite reductase. Electron transfer kinetics and charge storage. *Biochemistry 48*, 2828−2838.

(12) Rögner, M., Nixon, P. J., and Diner, B. A. (1990) Purification and characterization of photosystem I and photosystem II core complexes from wild-type and phycocyanin-deficient strains of the cyanobacterium *Synechocystis* PCC 6803. *J. Biol. Chem. 265*, 6189−6196.

(13) Barth, P., Guillouard, I., Sétif, P., and Lagoutte, B. (2000) Essential role of a single arginine of photosystem I in stabilizing the electron transfer complex with ferredoxin. *J. Biol. Chem. 275*, 7030−7036.

(14) Hurley, J. K., Hazzard, J. T., Martínez-Júlvez, M., Medina, M., Gómez-Moreno, C., and Tollin, G. (1999) Electrostatic forces involved in orienting *Anabaena* ferredoxin during binding to *Anabaena* ferredoxin-$NADP^+$ reductase: Site-specific mutagenesis, transient kinetic measurements, and electrostatic surface potentials. *Protein Sci. 8*, 1614−1622.

(15) Hurley, J. K., Faro, M., Brodie, T. B., Hazzard, J. T., Medina, M., Gomez-Moreno, C., and Tollin, G. (2000) Highly nonproductive complexes with *Anabaena* ferredoxin at low ionic strength are induced by nonconservative amino acid substitutions at Glu139 in *Anabaena* ferredoxin:$NADP^+$ reductase. *Biochemistry 39*, 13695−13702.

(16) Davidson, V. L. (2002) Chemically gated electron transfer. A means of accelerating and regulating rates of biological electron transfer. *Biochemistry 41*, 14633−14636.

(17) Sweeney, W. W., and Rabinowitz, J. C. (1980) Proteins containing 4Fe-4S clusters: An overview. *Annu. Rev. Biochem. 49*, 139−161.

(18) Blamey, J. M., Chiong, M., Lopez, C., and Smith, E. T. (2000) Purification and characterization of ferredoxin from the hyperthermophilic *Pyrococcus woesei*. *Anaerobe 6*, 285−290.

(19) Kamat, S. S., Williams, H. J., and Raushel, F. M. (2011) Intermediates in the transformation of phosphonates to phosphate by bacteria. *Nature 480*, 570−573.

(20) Reyntjens, B., Jollie, D. R., Stephens, P. J., Gao-Sheridan, H. S., and Burgess, B. K. (1997) Purification and characterization of a fixABCX-linked 2[4Fe-4S] ferredoxin from *Azotobacter vinelandii*. *J. Biol. Inorg. Chem. 2*, 595−602.

(21) Antonkine, M. L., Koay, M. S., Epel, B., Breitenstein, C., Gopta, O., Gärtner, W., Bill, E., and Lubitz, W. (2009) Synthesis and characterization of *de novo* designed peptides modelling the binding sites of [4Fe−4S] clusters in photosystem I. *Biochim. Biophys. Acta 1787*, 995−1008.

(22) Moser, C. C., Anderson, J. L. R., and Dutton, P. L. (2010) Guidelines for tunneling in enzymes. *Biochim. Biophys. Acta 1797*, 1573−1586.

(23) Najmudin, S., Gonzalez, P. J., Trincao, J., Coelho, C., Mukhopadhyay, A., Cerqueira, N. M. F. S., Romao, C. C., Moura, I., Moura, J. J. G., Brondino, C. D., and Romao, M. J. (2008) Periplasmic nitrate reductase revisited: A sulfur atom completes the sixth coordination of the catalytic molybdenum. *J. Biol. Inorg. Chem. 13*, 737−753.

(24) Bastian, N. R., Kay, C. J., Barber, M. J., and Rajagopalan, K. V. (1991) Spectroscopic Studies of the Molybdenum-Containing Dimethyl-Sulfoxide Reductase from *Rhodobacter-sphaeroides* F-Sp denitrificans. *J. Biol. Chem. 266*, 45−51.

(25) Benson, N., Farrar, J. A., McEwan, A. G., and Thomson, A. J. (1992) Detection of the optical bands of molybdenum(V) in DMSO reductase (*Rhodobacter capsulatus*) by low-temperature MCD spectroscopy. *FEBS Lett. 307*, 169−172.

(26) Bray, R. C., Adams, B., Smith, A. T., Richards, R. L., Lowe, D. J., and Bailey, S. (2001) Reactions of dimethylsulfoxide reductase in the presence of dimethyl sulfide and the structure of the dimethyl sulfide-modified enzyme. *Biochemistry 40*, 9810−9820.
(27) Finnegan, M. G., Hilton, J., Rajagopalan, K. V., and Johnson, M. K. (1993) Optical-Transitions of Molybdenum(V) in Glycerol-Inhibited DMSO Reductase from *Rhodobacter sphaeroides*. *Inorg. Chem. 32*, 2616−2617.
(28) Butler, C. S., Charnock, J. M., Bennett, B., Sears, H. J., Reilly, A. J., Ferguson, S. J., Garner, C. D., Lowe, D. J., Thomson, A. J., Berks, B. C., and Richardson, D. J. (1999) Models for molybdenum coordination during the catalytic cycle of periplasmic nitrate reductase from Paracoccus denitrificans derived from EPR and EXAFS spectroscopy. *Biochemistry 38*, 9000−9012.
(29) Cerqueira, N. M. F. S., Gonzalez, P. J., Brondino, C. D., Romao, M. J., Romao, C. C., Moura, I., and Moura, J. J. G. (2009) The effect of the sixth sulfur ligand in the catalytic mechanism of periplasmic nitrate reductase. *J. Comput. Chem. 30*, 2466−2484.